JACS
JOURNAL OF THE AMERICAN CHEMICAL SOCIETY
pubs.acs.org/JACS
Communication

# Co(II) Complex with a Covalently Attached Pendent Quinol Selectively Reduces $O_2$ to $H_2O$

Segun V. Obisesan, Cayla Rose, Byron H. Farnum, and Christian R. Goldsmith*

Cite This: https://doi.org/10.1021/jacs.2c08315
Read Online



**ABSTRACT:** A Co(II) complex with the polydentate quinol-containing ligand $H_2$qp1 acts as an efficient electrocatalyst for oxygen reduction. Without any additional electron−proton transfer mediators, the electrocatalysis is selective for $H_2O$; a related complex that substitutes a phenol for the quinol, conversely, instead produces mostly $H_2O_2$ under the same conditions. We propose that the ability of the redox-active quinol to donate two electrons impacts the product-determining step.



The oxygen reduction reaction (ORR) features prominently in many biological processes and proposed technologies for energy storage.[1] $O_2$ can be reduced either by two or four electrons to $H_2O_2$ or $H_2O$, respectively. $H_2O_2$ is vital to many industrial processes, making reactions that can readily prepare it from $O_2$ attractive, but this oxidant can degrade both biomolecules and the membranes used in fuel cells. Consequently, there is great interest in understanding the factors that favor the production of either $H_2O$ or $H_2O_2$ from $O_2$ and preparing catalysts and electrocatalysts that are highly selective for one over the other.

A number of first-row transition metal complexes have been explored as homogeneous electrocatalysts for ORR.[2−8] These include iron-porphyrin complexes, which resemble the cytochrome c oxidases essential for respiratory redox in mitochondria[9−17] and iron and cobalt complexes with dianionic ligands with $N_2O_2$ donor sets.[6,18−22] With respect to the cobalt-containing electrocatalysts, Anson and Stahl found that the addition of *para*-hydroquinone (quinol) was able to both accelerate the $O_2$ reduction and shift the product from mostly $H_2O_2$ to mostly $H_2O$.[19] In these reactions, the quinol is proposed to act as an electron−proton transfer mediator. Hooe et al. found that the addition of quinol likewise shifted the selectivity of a manganese-salen electrocatalyst for ORR toward $H_2O$.[23] Singha et al. subsequently grafted quinols to iron porphyrins, which were then attached to electrodes and used as heterogeneous electrocatalysts.[24] With these, the incorporation of a quinol was found to alter the mechanism of $O_2$ reduction relative to complexes with appended phenols, but the rates of oxygen reduction were similar. Further, both the quinol and phenol systems overwhelmingly produced $H_2O$.

Here, we report two cobalt-containing homogeneous electrocatalysts for ORR. These differ from earlier catalysts from the Machan and Stahl groups in that they feature neutral and potentially more highly coordinating ligands with $N_5O$ donor sets. The O-donor is, at best, loosely coordinated and comes from either a phenol or a quinol. We find that with these electrocatalysts the phenol-for-quinol substitution strongly impacts the product selectivity. When the O-donor is completely absent, the resultant cobalt complex performed poorly as an electrocatalyst for the ORR.

We prepared Co(II) complexes with *N*,*N*,*N*′-tris(2-pyridinylmethyl)-1,2-ethanediamine (trispicen),[25] *N*-(2-hydroxybenzyl)-*N*,*N*′,*N*′-tris(2-pyridinylmethyl)-1,2-ethanediamine (Hpp), and *N*-(2,5-dihydroxybenzyl)-*N*,*N*′,*N*′-tris(2-pyridinylmethyl)-1,2-ethanediamine ($H_2$qp1, Scheme 1). We had previously synthesized $H_2$qp1 and used it as a component in a redox-responsive magnetic resonance imaging contrast agent and in two functional mimics of superoxide dismutase.[26−28] The complexation reactions between $Co^{II}(OTf)_2$ and the ligands were all performed in MeCN. Adding ether precipitates the following products in moderate yields: [Co(trispicen)]-$(OTf)_2$ (**1**, 72%), [Co(Hpp)]$(OTf)_2$ (**2**, 55%), and [Co-$(H_2$qp1)]$(OTf)_2$ (**3**, 76%). Although we have been unable thus far to structurally characterize the complexes, we

**Scheme 1. Structures of the Polydentate Ligands**

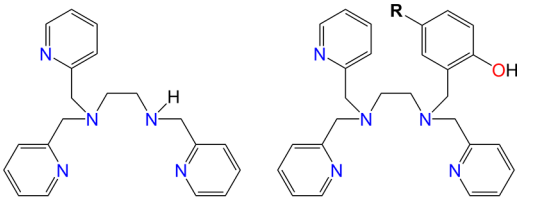


[Co(trispicen)](OTf)$_2$ (**1**)
[Co(Hpp)](OTf)$_2$ (**2**)
[Co($H_2$qp1)](OTf)$_2$ (**3**)

**Received:** August 5, 2022

confirmed their identities and purities by elemental analysis, with coordination of the ligands being corroborated by mass spectrometry (MS). Solid-state magnetic susceptibility measurements indicate that each complex contains high-spin Co(II).[29]

Cyclic voltammetry (CV) analysis of **1**, **2**, and **3** in MeCN under $N_2$ reveals that the three cobalt complexes each have a quasi-reversible feature at approximately −0.45 vs $Fc^+/Fc$ (Table 1, Figures S11−S13). Given the similarities of these

**Table 1. Summary of Electrochemical Data for 1, 2, and 3**[a]

| complex | $E_{1/2}$ for Co(III/II) (V vs $Fc^+/Fc$) | additional redox events (V vs $Fc^+/Fc$) |
|---|---|---|
| **1** | −0.41 | N.A. |
| **2** | −0.47 | N.A. |
| **3** | −0.49 | 0.61($E_{pa}$), 0.55, 0.07 ($E_{pc}$) |

[a]All data were acquired in MeCN under $N_2$ with 100 mM $[Bu_4N][PF_6]$ as a supporting electrolyte and a 25 mV/s scan rate.

potentials, we assign these to Co(III/II) redox events. The presence of a phenolic group on the ligand shifts the potential slightly more negative. Complex **3** has additional redox events: a single $2e^-$ oxidation wave at 0.61 V and what appears to be two $1e^-$ reduction features at 0.55 and 0.07 V, respectively (Figure S13). The Co(III/II) redox features for **2** and **3** do not significantly shift in the presence of either AcOH or acetate buffer. The Co(III/II) redox event in **1**, however, shifts by −0.28 V (Figure S11), suggesting a change in the coordination environment of the metal center.

When the electrochemistry is performed in the presence of 100 mM acetate buffer (50 mM AcOH/50 mM NaOAc) and $O_2$ in MeCN, the reversibility is lost, and the current markedly increases around the Co(III/II) potential for **2** and **3** (Figure 1, Figure S14) but not **1**. The results indicate that **2** and **3** are both able to bind to $O_2$ and act as electrocatalysts. We were unable to observe a current increase for **1** beyond the overlapping $O_2$ reduction by the glassy carbon electrode near the $E_{1/2}$ of the Co(III/II). In nonbuffered solutions containing 50 mM AcOH, we observe a catalytic current for **1** that is too weak to allow for the measurement of accurate kinetic data (Figure S15). A proton donor-dependent voltage response was seen with **2**. At 0 mM AcOH under $O_2$ saturation, the $E_{p/2}$ is equal to the $E_{1/2}$. Increasing the proton concentration from 0 to 200 mM led to a positive shift of 51 mV, suggesting the protonation and potential stabilization of the intermediate formed from the first reduction.[6,30] The abilities of **2** and **3** to function at acid concentrations as high as 200 mM are notable; such conditions have deactivated other molecular electrocatalysts for the ORR.[8] We do observe slightly enhanced currents under $O_2$ in the absence of acetic acid for both **2** and **3**; we attribute this to the phenolic portions of the ligands acting as proton sources.

The turnover frequencies (TOFs) for both catalysts were determined using scan rate-independent CV data to estimate $k_{obs}$ from the $i_c/i_p$ ratio and the $n_{cat}$ determined from RRDE studies (*vide infra*), where $i_c$ is the plateau catalytic current and $i_p$ is the peak current for **2** or **3** under $N_2$ (eq 1).[31] $k_{obs}$ was estimated to be the maximum TOF.

$$\frac{i_c}{i_p} = \frac{n}{0.4463}\sqrt{\frac{RTk_{obs}}{F\nu}} \quad (1)$$

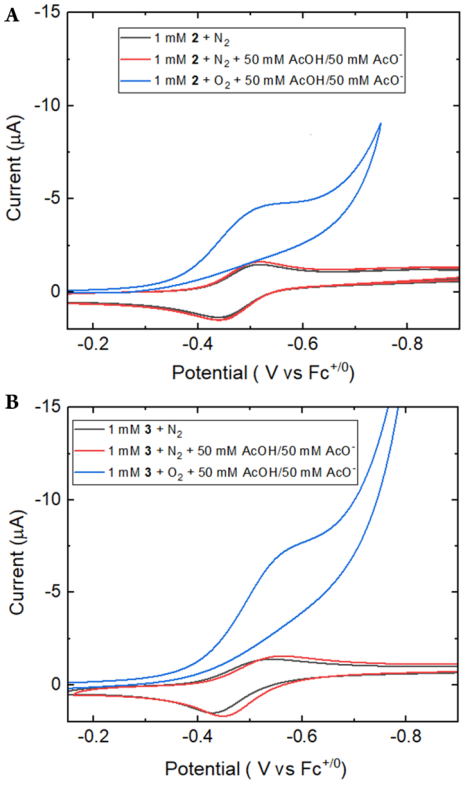


**Figure 1.** Electrocatalytic dioxygen reduction by **2** and **3** in MeCN. (A) CV of **2** under $N_2$ and $O_2$ with and without 100 mM acetate buffer (50 mM AcOH/50 mM NaOAc). (B) CV of **3** under $N_2$ and $O_2$ with and without 100 mM acetate buffer. All potentials are vs $Fc^+/Fc$.

With 6.3 mM $O_2$[32] and 400 mM acetate buffer (200 mM AcOH/200 mM NaOAc), the TOFs for $O_2$ reduction are 0.16 $s^{-1}$ for **2** and 0.154 $s^{-1}$ for **3**. These TOF values are weighted averages of the observed rate constants for the reactions that reduce $O_2$ to $H_2O$ and $H_2O_2$. Attempts to corroborate these values with foot-of-the-wave analysis failed, suggesting that the first chemical step in the mechanism is not rate-determining. The effective overpotentials for the catalysts were determined through well-established methodology and measurements in buffered systems containing acetate buffer.[5] For **2** and **3**, the effective overpotentials for reduction to $H_2O$ were 310 and 333 mV, respectively.

Electrocatalysis with **2** and **3** was investigated as a function of [AcOH], $[O_2]$, and [Co], where [Co] is the concentration of **2** or **3** (Figures S16−S28). In the case of **3**, $k_{obs}$ is linearly dependent on [AcOH], $[O_2]$, and [Co]. When [AcOH] exceeds 50 mM, $k_{obs}$ becomes independent of acid concentration, with a limiting value of $k_{obs}$ = 0.33 $s^{-1}$ (Figure S24). This observation indicates two rate-limiting regimes. A linear fit to the [AcOH]-dependent region yields a slope of 8.1 $M^{-1}$ $s^{-1}$ and an intercept of 0.052 $s^{-1}$. This intercept is thus $k_{obs}$ for $O_2$ reduction by **3** in the absence of external acid. We attribute the residual activity to the acidic −OH groups of the $H_2$qp1 ligand. The linear dependence of $k_{obs}$ on $[O_2]$ obtained in excess [AcOH] yields a slope of 48 $M^{-1}$ $s^{-1}$. Multiplying this value by $[O_2]$ (6.3 mM) yields $k_{obs}$ = 0.30 $s^{-1}$, which is identical within error to that found in the acid-independent region for $k_{obs}$ vs [AcOH]. These data indicate two chemical steps. The first is dependent on [AcOH], whereas the second depends on $O_2$.


https://doi.org/10.1021/jacs.2c08315
J. Am. Chem. Soc. XXXX, XXX, XXX−XXX

With **2**, $k_{obs}$ shows a strong linear dependence on [AcOH] until it exceeds 100 mM (Figure S17). Above this concentration, $k_{obs}$ appears to approach a limiting value, but unlike what is observed for **3**, a clear limit is never reached. A fit to the linear region yielded a slope of 5.6 $M^{-1}$ $s^{-1}$ for the acid-dependent rate constant and an intercept of 0.047 $s^{-1}$ in the absence of AcOH.

The selectivities of **2** and **3** for $H_2O$ and $H_2O_2$ differ substantially. The product selectivity was assessed using two different methods: a rotating ring-disk electrode (RRDE, Figures S29−S33) and a colorimetric assay with titanium(IV) oxysulfate, [$Ti^{IV}(O)SO_4$] (Figures S34−S37). With 50 mM AcOH, **2** favors the production of $H_2O_2$ from $O_2$; $H_2O_2$ accounts for 89 ± 7% of the products as assessed by RRDE ($n_{cat}$ = 2.2) and 62% of the products as assessed by the assay. Although the concentration of AcOH strongly influences the rate of ORR, it does not impact the selectivity. Increasing [AcOH] to 200 mM results in 83 ± 5% selectivity for $H_2O_2$, as assessed by RRDE. Catalyst **3**, conversely, selectively converts $O_2$ into $H_2O$. RRDE again suggests a higher amount of $H_2O_2$ (25 ± 7%, $n_{cat}$ = 3.5) than the Ti(IV) assay (<4%). Such discrepancies between these two techniques have been previously noted and typically result when the catalysts can further reduce $H_2O_2$.[6] In the assay, the $H_2O_2$ remains in proximity with the electrocatalyst, enabling its further reduction to $H_2O$. In the RRDE measurements, conversely, the $H_2O_2$ diffuses away from the electrocatalyst before it can get reduced through secondary reactions, weighting the observed selectivity more toward $H_2O_2$. CV studies with various concentrations of $H_2O_2$ confirm that **2** and **3** can indeed further reduce $H_2O_2$ to $H_2O$ (Figure S38).

To determine the impact of an added electron−proton transfer mediator on the selectivity and rate of the electrocatalyzed ORR, we studied the reactions with 0.5−2.5 mM *para*-hydroquinone present as a cocatalyst. Although accurately determining the TOFs of a catalyst/cocatalyst mixture is challenging,[19,23] there appears to be a first-order dependence on the quinol concentration for **2**, as evidenced by the enhanced catalytic current around the Co(III/II) redox couple (Figure S39). With 2.5 mM quinol, **2** now favors the production of $H_2O$, which accounts for 61 ± 9% and 85% of the products as assessed by RRDE (Figure S40) and the titanium assay (Figure S41), respectively. Catalyst **3** also becomes more active upon the addition of quinol (Figure S41), and its selectivity for $H_2O$ measured by RRDE improves to 89 ± 6% (Figure S42). As seen by Anson et al., the added quinol cooperatively shuttles electrons and protons to the species on the catalytic cycle, facilitating the complete reduction of $O_2$ to $H_2O$.[19]

Although compounds **2** and **3** highly resemble each other in most aspects, we believe that the ability of the quinol in **3** to donate two electrons and two protons alters the mechanism for ORR and shifts the product selectivity from $H_2O_2$ to $H_2O$. Given that both complexes are present in their reduced Co(II) forms, we believe that an equilibrium with $O_2$ in the bulk solution produces Co(III)-superoxo complexes that act as the active catalysts (Scheme 2). The reduction of the Co(III)-superoxo complex to a putative Co(III)-peroxo species is the first step. The Co(III)-peroxo then reacts with AcOH with rate constants of $k_1$ = 5.6 and 8.1 $M^{-1}$ $s^{-1}$ for **2** and **3**, respectively. This step is also proposed to be product-determining. For **3**, external protonation coupled with rapid PCET from the quinol group yields $H_2O$ as the major product as well as a Co(III)−OH-*para*-quinone species. For **2**, both external and internal protonation of Co(III)-peroxo yields $H_2O_2$ as the major product as well as a Co(III)-phenolate complex. Subsequent PCET reactions at the electrode surface regenerate the starting Co(II) complexes for both catalysts, with subsequent $O_2$ coordination regenerating the Co(III)-superoxo complexes in the final step.

**Scheme 2. Proposed Mechanisms for the Electrocatalysis Performed by 3 in the Absence of Additional Quinol**

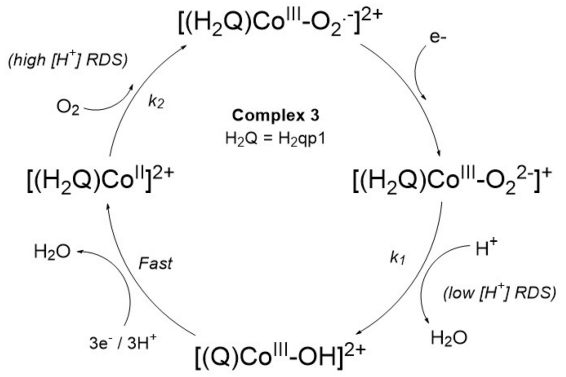


The overall mechanism represents an ECEC pathway in which either of the two chemical steps can be rate-limiting depending on the acid concentration.[33,34] At low [AcOH], the rate-determining step corresponds to $k_1$, but as [AcOH] increases, the RDS switches to $O_2$ coordination. Importantly, many reported electrocatalysts for ORR initially enter the catalytic cycle in an oxidized form (i.e., Co(III)). With these catalysts, $O_2$ coordination typically is the first step after reduction of the catalyst. In the present study, the catalysts instead start in the reduced state, and $O_2$ coordination occurs as the final step in the catalytic cycle. The regenerated Co(III)-superoxo complex is then reduced at the electrode surface. Further evidence for the order of protonation and $O_2$ coordination steps comes from the positive shift in $E_{cat/2}$ with [AcOH], a result only supported by protonation occurring as the first step (Figure S46).

This mechanism also presents a challenge in that the peak current ($i_p$) used to calculate $i_c/i_p$ and determine $k_{obs}$ is that of the Co(II) complex under $N_2$, rather than the Co(III)-superoxo. Given that we do not know the equilibrium constant for $O_2$ coordination with Co(II), we cannot know the concentration of Co(III)-superoxo in the bulk solution. We anticipate that this equilibrium is quite small, such that [Co(II)] > [Co(III)-superoxo]. Consequently, the $i_c/i_p$ values and corresponding $k_{obs}$ values here should be considered lower limits for the true values.

In comparison to other molecular electrocatalysts, **3** stands out for being selective for $H_2O$ at a relatively low overpotential. Cobalt-containing catalysts can perform at lower overpotentials than iron-containing complexes, sometimes as low as 90 mV, but are generally much more selective for $H_2O_2$ and have lower TOFs.[5,18,19] Although other catalysts are more selective for $H_2O$ than **3**, these typically have much higher overpotentials exceeding 0.7 V.[3,6−8,17,31,35,36]

In conclusion, we find that installing a phenol in a neutral pentadentate N-donor ligand can enable a formerly inactive cobalt complex to serve as an effective electrocatalyst for ORR. Slightly changing the phenol into a quinol markedly improves


https://doi.org/10.1021/jacs.2c08315
J. Am. Chem. Soc. XXXX, XXX, XXX−XXX

the selectivity for $H_2O$ over $H_2O_2$. The presence of additional, noncovalently bound quinol amplifies these benefits.

## ■ ASSOCIATED CONTENT

### Supporting Information

The Supporting Information is available free of charge at https://pubs.acs.org/doi/10.1021/jacs.2c08315.

Discussions of experimental details and ECEC mechanisms for ORR electrocatalysis, figures of mass spectra, IR spectra, ESI MS data, CV curves, plots of cathodic and anodic peak currents, rotating ring disc electrode data, and UV/vis spectra, and tables of cbserved rate constants for oxygen reduction (PDF)

## ■ AUTHOR INFORMATION


### Corresponding Author

**Christian R. Goldsmith** − *Department of Chemistry and Biochemistry, Auburn University, Auburn, Alabama 36849, United States;* orcid.org/0000-0001-7293-1267; Email: crgoldsmith@auburn.edu

### Authors

**Segun V. Obisesan** − *Department of Chemistry and Biochemistry, Auburn University, Auburn, Alabama 36849, United States*

**Cayla Rose** − *Department of Chemistry and Biochemistry, Auburn University, Auburn, Alabama 36849, United States*

**Byron H. Farnum** − *Department of Chemistry and Biochemistry, Auburn University, Auburn, Alabama 36849, United States*

Complete contact information is available at: https://pubs.acs.org/10.1021/jacs.2c08315


### Notes

The authors declare no competing financial interest.

## ■ ACKNOWLEDGMENTS

The research described here was financially supported by Auburn University and two grants from the National Science Foundation (NSF-CHE-1662875 and NSF-CHE-1954336).

## ■ REFERENCES


(1) Solomon, E. I.; Stahl, S. S. Introduction: Oxygen Reduction and Activation in Catalysis. *Chem. Rev.* **2018**, *118* (5), 2299−2301.

(2) Machan, C. W. Advances in the Molecular Catalysis of Dioxygen Reduction. *ACS Catal.* **2020**, *10* (4), 2640−2655.

(3) Hooe, S. L.; Rheingold, A. L.; Machan, C. W. Electrocatalytic Reduction of Dioxygen to Hydrogen Peroxide by a Molecular Manganese Complex with a Bipyridine-Containing Schiff Base Ligand. *J. Am. Chem. Soc.* **2018**, *140* (9), 3232−3241.

(4) Wang, Y.-H.; Schneider, P. E.; Goldsmith, Z. K.; Mondal, B.; Hammes-Schiffer, S.; Stahl, S. S. Brønsted Acid Scaling Relationships Enable Control Over Product Selectivity from $O_2$ Reduction with a Mononuclear Cobalt Porphyrin Catalyst. *ACS Cent. Sci.* **2019**, *5* (6), 1024−1034.

(5) Pegis, M. L.; Wise, C. F.; Martin, D. J.; Mayer, J. M. Oxygen Reduction by Homogeneous Molecular Catalysts and Electrocatalysts. *Chem. Rev.* **2018**, *118* (5), 2340−2391.

(6) Cook, E. N.; Dickie, D. A.; Machan, C. W. Catalytic Reduction of Dioxygen to Water by a Bioinspired Non-Heme Iron Complex via a 2+2 Mechanism. *J. Am. Chem. Soc.* **2021**, *143* (40), 16411−16418.

(7) Wang, L.; Gennari, M.; Cantú Reinhard, F. G.; Gutiérrez, J.; Morozan, A.; Philouze, C.; Demeshko, S.; Artero, V.; Meyer, F.; de Visser, S. P.; Duboc, C. A Non-Heme Diiron Complex for (Electro)catalytic Reduction of Dioxygen: Tuning the Selectivity through Electron Delivery. *J. Am. Chem. Soc.* **2019**, *141* (20), 8244−8253.

(8) Passard, G.; Ullman, A. M.; Brodsky, C. N.; Nocera, D. G. Oxygen Reduction Catalysis at a Dicobalt Center: The Relationship of Faradaic Efficiency to Overpotential. *J. Am. Chem. Soc.* **2016**, *138* (9), 2925−2928.

(9) Martin, D. J.; Mayer, J. M. Oriented Electrostatic Effects on $O_2$ and $CO_2$ Reduction by a Polycationic Iron Porphyrin. *J. Am. Chem. Soc.* **2021**, *143* (30), 11423−11434.

(10) Brezny, A. C.; Johnson, S. I.; Raugei, S.; Mayer, J. M. Selectivity-Determining Steps in $O_2$ Reduction Catalyzed by Iron(tetramesitylporphyrin). *J. Am. Chem. Soc.* **2020**, *142* (9), 4108−4113.

(11) Pegis, M. L.; Martin, D. J.; Wise, C. F.; Brezny, A. C.; Johnson, S. I.; Johnson, L. E.; Kumar, N.; Raugei, S.; Mayer, J. M. Mechanism of Catalytic $O_2$ Reduction by Iron Tetraphenylporphyrin. *J. Am. Chem. Soc.* **2019**, *141* (20), 8315−8326.

(12) Rigsby, M. L.; Wasylenko, D. J.; Pegis, M. L.; Mayer, J. M. Medium Effects Are as Important as Catalyst Design for Selectivity in Electrocatalytic Oxygen Reduction by Iron−Porphyrin Complexes. *J. Am. Chem. Soc.* **2015**, *137* (13), 4296−4299.

(13) Wasylenko, D. J.; Rodríguez, C.; Pegis, M. L.; Mayer, J. M. Direct Comparison of Electrochemical and Spectrochemical Kinetics for Catalytic Oxygen Reduction. *J. Am. Chem. Soc.* **2014**, *136* (36), 12544−12547.

(14) Carver, C. T.; Matson, B. D.; Mayer, J. M. Electrocatalytic Oxygen Reduction by Iron Tetra-arylporphyrins Bearing Pendant Proton Relays. *J. Am. Chem. Soc.* **2012**, *134* (12), 5444−5447.

(15) Singha, A.; Dey, A. Hydrogen Atom Abstraction by Synthetic Heme Ferric Superoxide and Hydroperoxide species. *Chem. Commun.* **2019**, *55* (39), 5591−5594.

(16) Brezny, A. C.; Nedzbala, H. S.; Mayer, J. M. Multiple Selectivity-Determining Mechanisms of $H_2O_2$ Formation in Iron Porphyrin-Catalysed Oxygen Reduction. *Chem. Commun.* **2021**, *57* (10), 1202−1205.

(17) Pegis, M. L.; McKeown, B. A.; Kumar, N.; Lang, K.; Wasylenko, D. J.; Zhang, X. P.; Raugei, S.; Mayer, J. M. Homogenous Electrocatalytic Oxygen Reduction Rates Correlate with Reaction Overpotential in Acidic Organic Solutions. *ACS Cent. Sci.* **2016**, *2* (11), 850−856.

(18) Wang, Y.-H.; Pegis, M. L.; Mayer, J. M.; Stahl, S. S. Molecular Cobalt Catalysts for $O_2$ Reduction: Low-Overpotential Production of $H_2O_2$ and Comparison with Iron-Based Catalysts. *J. Am. Chem. Soc.* **2017**, *139* (46), 16458−16461.

(19) Anson, C. W.; Stahl, S. S. Cooperative Electrocatalytic $O_2$ Reduction Involving Co(salophen) with *p*-Hydroquinone as an Electron−Proton Transfer Mediator. *J. Am. Chem. Soc.* **2017**, *139* (51), 18472−18475.

(20) Nichols, A. W.; Cook, E. N.; Gan, Y. J.; Miedaner, P. R.; Dressel, J. M.; Dickie, D. A.; Shafaat, H. S.; Machan, C. W. Pendent Relay Enhances $H_2O_2$ Selectivity during Dioxygen Reduction Mediated by Bipyridine-Based Co−$N_2O_2$ Complexes. *J. Am. Chem. Soc.* **2021**, *143* (33), 13065−13073.

(21) Nichols, A. W.; Kuehner, J. S.; Huffman, B. L.; Miedaner, P. R.; Dickie, D. A.; Machan, C. W. Reduction of Dioxygen to Water by a Co($N_2O_2$) Complex with a 2,2′-Bipyridine Backbone. *Chem. Commun.* **2021**, *57* (4), 516−519.

(22) Wang, Y.-H.; Goldsmith, Z. K.; Schneider, P. E.; Anson, C. W.; Gerken, J. B.; Ghosh, S.; Hammes-Schiffer, S.; Stahl, S. S. Kinetic and Mechanistic Characterization of Low-Overpotential, $H_2O_2$-Selective Reduction of $O_2$ Catalyzed by $N_2O_2$-Ligated Cobalt Complexes. *J. Am. Chem. Soc.* **2018**, *140* (34), 10890−10899.

(23) Hooe, S. L.; Cook, E. N.; Reid, A. G.; Machan, C. W. Non-Covalent Assembly of Proton Donors and *p*-Benzoquinone Anions for Co-Electrocatalytic Reduction of Dioxygen. *Chem. Sci.* **2021**, *12* (28), 9733−9741.

(24) Singha, A.; Mondal, A.; Nayek, A.; Dey, S. G.; Dey, A. Oxygen Reduction by Iron Porphyrins with Covalently Attached Pendent Phenol and Quinol. *J. Am. Chem. Soc.* **2020**, *142* (52), 21810−21828.

(25) Mialane, P.; Nivorojkine, A.; Pratviel, G.; Azéma, L.; Slany, M.; Godde, F.; Simaan, A.; Banse, F.; Kargar-Grisel, T.; Bouchoux, G.; Sainton, J.; Horner, O.; Guilhem, J.; Tchertanova, L.; Meunier, B.; Girerd, J.-J. Structures of Fe(II) Complexes with *N,N,N'*-Tris(2-pyridylmethyl)ethane-1,2-diamine Type Ligands. Bleomycin-like DNA Cleavage and Enhancement by an Alkylammonium Substituent on the N' Atom of the Ligand. *Inorg. Chem.* **1999**, *38* (6), 1085−1092.
(26) Yu, M.; Ambrose, S. L.; Whaley, Z. L.; Fan, S.; Gorden, J. D.; Beyers, R. J.; Schwartz, D. D.; Goldsmith, C. R. A Mononuclear Manganese(II) Complex Demonstrates a Strategy to Simultaneously Image and Treat Oxidative Stress. *J. Am. Chem. Soc.* **2014**, *136* (37), 12836−12839.
(27) Senft, L.; Moore, J. L.; Franke, A.; Fisher, K. R.; Scheitler, A.; Zahl, A.; Puchta, R.; Fehn, D.; Ison, S.; Sader, S.; Ivanović-Burmazović, I.; Goldsmith, C. R. Quinol-Containing Ligands Enable High Superoxide Dismutase Activity by Modulating Coordination Number, Charge, Oxidation States and Stability of Manganese Complexes throughout Redox Cycling. *Chem. Sci.* **2021**, *12* (31), 10483−10500.
(28) Ward, M. B.; Scheitler, A.; Yu, M.; Senft, L.; Zillmann, A. S.; Gorden, J. D.; Schwartz, D. D.; Ivanović-Burmazović, I.; Goldsmith, C. R. Superoxide Dismutase Activity Enabled by a Redox-Active Ligand rather than Metal. *Nat. Chem.* **2018**, *10* (12), 1207−1212.
(29) Drago, R. S.*Physical Methods for Chemists*, 2nd ed.; Surfside Scientific Publishers: Gainesville, FL, 1992.
(30) Artero, V.; Saveant, J.-M. Toward the Rational Benchmarking of Homogeneous $H_2$-Evolving Catalysts. *Energy Environ. Sci.* **2014**, *7* (11), 3808−3814.
(31) Costentin, C.; Savéant, J.-M. Towards an Intelligent Design of Molecular Electrocatalysts. *Nat. Rev. Chem.* **2017**, *1* (11), 0087.
(32) Li, Q.; Batchelor-McAuley, C.; Lawrence, N. S.; Hartshorne, R. S.; Compton, R. G. Anomalous Solubility of Oxygen in Acetonitrile/Water Mixture Containing Tetra-*n*-butylammonium Perchlorate Supporting Electrolyte; the Solubility and Diffusion Coefficient of Oxygen in Anhydrous Acetonitrile and Aqueous Mixtures. *J. Electroanal. Chem.* **2013**, *688*, 328−335.
(33) Rountree, E. S.; McCarthy, B. D.; Eisenhart, T. T.; Dempsey, J. L. Evaluation of Homogeneous Electrocatalysts by Cyclic Voltammetry. *Inorg. Chem.* **2014**, *53* (19), 9983−10002.
(34) Costentin, C.; Savéant, J.-M. Multielectron, Multistep Molecular Catalysis of Electrochemical Reactions: Benchmarking of Homogeneous Catalysts. *ChemElectroChem* **2014**, *1* (7), 1226−1236.
(35) Costentin, C.; Robert, M.; Savéant, J.-M. Current Issues in Molecular Catalysis Illustrated by Iron Porphyrins as Catalysts of the $CO_2$-to-CO Electrochemical Conversion. *Acc. Chem. Res.* **2015**, *48* (12), 2996−3006.
(36) Wang, Y.-H.; Mondal, B.; Stahl, S. S. Molecular Cobalt Catalysts for $O_2$ Reduction to $H_2O_2$: Benchmarking Catalyst Performance via Rate−Overpotential Correlations. *ACS Catal.* **2020**, *10* (20), 12031−12039.


https://doi.org/10.1021/jacs.2c08315
*J. Am. Chem. Soc.* XXXX, XXX, XXX−XXX